Published in: Optics Letters (2006), vol. 31, iss. 7, pp. 990-992
Status: Postprint (Author's version)

Space-domain lock-in amplifier based on a liquid-crystal spatial light modulator

Gregory P. Lousberg, Lars D. A. Lundeberg, Dmitri L. Boiko, and Eli Kapon

Ecole Polytechnique Fédérale de Lausanne, Laboratory of Physics of Nanostructures, CH-1015 Lausanne, Switzerland

Abstract

We present a two-dimensional (2D) spatial lock-in amplifier that provides a contrast ratio of more than 10,000:1 for transmitted and blocked intensity patterns using a conventional liquid-crystal spatial light modulator. The device is based on spatial-domain modulation-demodulation of intensity patterns under coherent imaging conditions. The operation of the 2D lock-in amplifier is illustrated by implementing Young's double-slit arrangement for measurements of the mutual coherence between individual emitters of a 2D phase-coupled array of vertical cavity surface emitting lasers.

At present, commercially available liquid-crystal spatial light modulators (SLMs) comprise up to 512 X512 individually addressable phase-retarding electro-optic cells and provide a space-bandwidth product of ~10^5. SLMs have found applications such as precise patterning and shaping of optical beams, [1,2] as well as information processing and optical tweezers, and they allow the implementation of dynamically tunable diffraction gratings.[4,5]

The spatial resolution of a SLM-based system is limited by the contrast of the intensity pattern modulation and is not as high as the space-bandwidth product of the liquid-crystal SLM itself. [6,7] Conventional arrangements for intensity pattern modulation with a phase-only SLM are based on a pair of a crossed polarizer and an analyzer. Although a narrow beam focused on an individual pixel of a one-dimensional (1D) array liquid-crystal modulator can yield a 30 dB contrast of intensity modulation, the modulation contrast for a broad optical beam ranges from 60:1 to 250:1.[1,6]

In this Letter we demonstrate a two-dimensional (2D) lock-in amplifier with a contrast ratio of more than 10^4:1 for dynamic aperturing of broad-area optical beams utilizing a pixelated SLM of specified contrast 200:1. The lock-in amplifier is based on spatial modulation of selective image domains followed by synchronous spatial filtering and detection. We illustrate an application of our method by generating a dynamically configurable Young's double-slit arrangement and measuring the degree of coherence between individual emitters of a 2D phase-coupled array of vertical cavity surface emitting lasers (VCSELs).[10]

We use a parallel-aligned nematic liquid-crystal phase-only SLM from Boulder Nonlinear Systems, Inc. (Model 128-SA-N-1000). The device incorporates an active array of 5.12 mm × 5.12 mm area and operates in a double-path reflective configuration. The active array has 128 × 128 pixels on $\Lambda_{SLM} = 40\ \mu$m pitch that are individually addressed with 128 gray levels.

The phase retardance was calibrated with the method of crossed polarizers[8] at $\lambda = 940$ nm wave-length. The measured modulation range of the phase retardance was 1.6λ, while the modulation contrast ratio was 70:1. Due to the SLM cell fill factor of 60%, the transmittance was limited to 36% of the diffraction efficiency into the zeroth order of the uniform SLM pattern.

Apart from possible misalignment of polarizers and parasitic backreflections, the modulation contrast is degraded by nonuniformity of the modulation pattern. Nonuniformities due to variations of the SLM optical thickness and modulation characteristics of the pixels can be partially compensated for by individual pixel calibration. On the other hand, one cannot compensate for depolarization due to light diffraction and fringing fields at pixel edges. Even with individually optimized cell parameters, the best contrast ratio achievable with the

Published in: Optics Letters (2006), vol. 31, iss. 7, pp. 990-992
Status: Postprint (Author's version)

standard technique of crossed polarizers is of the order of 100:1. However, SLM applications such as spatial coherence measurements demand higher contrast. For example, a contrast of 10^4:1 is needed to achieve a signal to noise (S/N) ratio of 100:1 in the far-field intensity distribution of a single element from a 10 × 10 element VCSEL array.

As an alternative to the crossed polarizer arrangement, it has been pointed out that spatially varying the amplitude of a 1D sawtooth phase grating can be used to control the diffracted light-intensity pattern. However, the reported contrast ratio in the zeroth diffraction order was only 50:1.

To improve the modulation contrast, we operate at the Nyquist limit of the spatial SLM frequency and use the first diffraction order. A 2D binary checkerboard phase pattern introducing a π-phase shift between neighboring SLM pixels was applied to a selected domain of a broad optical beam polarized along the extraordinary SLM axis. Under such modulation, the most important harmonics are of 0, $1/2\Lambda_{SLM}$, and $1/\Lambda_{SLM}$ spatial frequencies along the SLM grid directions. The long-scale nonuniformities of the SLM as well as the uniformly modulated domains contribute mainly to the zeroth diffraction order. The modulation features related to the pixelation of the SLM are centered at the $1/\Lambda_{SLM}$ spatial harmonics, and only the out-of-phase modulated part of the beam is diffracted into the four first-order principal lobes centered at spatial frequencies of $1/2\Lambda_{SLM}$. Spatial filtering of these lobes then results in selective transmission of the checkerboard phase-modulated image domains. Subsequent imaging and detection on a CCD camera thus yield a 2D spatial lock-in amplifier with an improved S/N ratio between the transmitted and the blocked intensity patterns.

Fig. 1: *Schematic of the 2D lock-in amplifier for spatial coherence measurements in VCSEL arrays. SLM, spatial light modulator; DP, Dove prism; WP, wave plate; BS, beam splitter; P1,P2, polarizers; A, aperture; CCD, camera; IR, iris diaphragm; M, mirror; f1, microscope objective (f1 = 8.55 mm, NA=0.4); f2-f4, lenses (f2 = 400, f3 = 300, and f4 = 163 mm). Distances a and b are 215 and 600 mm, respectively.*

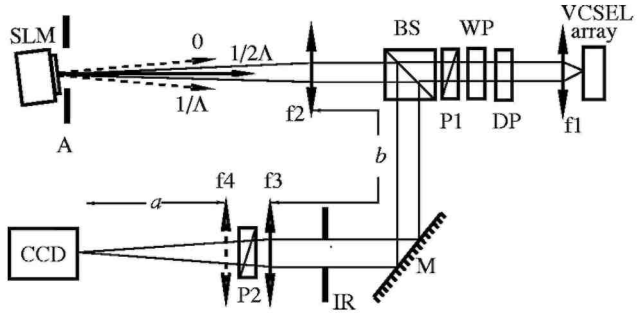

A simple analysis based on 2D Fourier series expansion shows that our pixelated SLM diffracts 51% of the intensity of the incident polarized beam into the first-order lobes. The transmission of such a 2D spatial lock-in amplifier can thus be higher than that of a conventional modulator based on two crossed polarizers and the zeroth diffraction order of the uniform SLM pattern.

Our experimental setup is shown in Fig. 1. The near field (NF) of the light source (we use a VCSEL array emitting at 940 nm wavelength) is imaged onto the SLM using a 4-*f* optical length system (lenses *f*1-*f*2). A Dove prism rotates the NF image, and a half-wave plate adjusts the polarization. To reduce depolarization effects, the axis of polarizer P1 is oriented parallel to the SLM's extraordinary axis and to the vertical axis of beam splitter BS1. Aperture A suppresses parasitic backreflections and scattering.

After the SLM, the NF pattern with selectively out-of-phase modulated domains is directed towards the CCD camera by beam splitter BS1. The iris diaphragm serves as a spatial filter located at the back focal plane of the *f*2 lens, filtering out only one principal lobe of the first diffraction order of the checkerboard SLM pattern. The NF domains with the out-of-phase modulation are imaged onto the CCD camera by lens *f*3. Polarizer P2 improves the modulation contrast by blocking the unintentional orthogonal polarization component. The far-field (FF) pattern is reconstructed on the CCD camera by introducing removable lens *f*4.

The contrast, defined as the ratio between intensities obtained with checkerboard and uniform SLM patterns, was

Published in: Optics Letters (2006), vol. 31, iss. 7, pp. 990-992
Status: Postprint (Author's version)

measured at the CCD camera. The checkerboard pattern used was of gray levels 42 and 62, providing a π-phase shift between neighboring SLM pixels. Figure 2 shows the intensity modulation contrast as a function of the gray level of the uniform pattern impressed on the SLM. Inhomogeneities of the actual phase retardation profile across the SLM with such a uniform pattern reduce the contrast. Thus the contrast minimum at intermediate gray levels is caused by variation of the modulation characteristics of the individual SLM pixels. At a gray level of 0, the contrast is high, as the SLM cells are not biased and all the liquid-crystal molecules are oriented along cell directors. At a gray level of 128, the contrast reaches the highest ratio of 11 000:1. At this level, the voltage applied to the SLM cells saturates the modulation curves of the individual pixels by orienting all the liquid-crystal molecules along the electric field. The uniform patterns of this gray level were used for blocking selected image domains.

To illustrate the use of a SLM-based 2D lock-in amplifier, we implement a dynamically configurable Young's double-slit arrangement for spatial coherence measurements across a phase-locked array of VCSELs. The visibility of Young's interference fringes was previously utilized to characterize coherence across 1D phase-coupled diode laser arrays. ' In those experiments, an opaque screen with a double slit was mechanically translated in one direction across a beam. The lock-in amplifier that we propose allows characterization of the 2D distribution of the spatial degree of coherence with no mechanically moving parts.

The studied 2D phase-coupled VCSEL array incorporated 10 × 10 elements defined by patterning the upper Bragg reflector and emitting at 940 nm wavelength. The 5μm × 5 μm unit cells of the array each containing one VCSEL, were imaged onto domains containing 6X6 SLM pixels. Pairs of such VCSELs were selected by modulating corresponding domains on the SLM with the checkerboard out-of-phase pattern to accomplish the space-domain lock-in operation.

Fig. 2: *Contrast ratio of the lock-in amplifier as a function of the gray level of the uniform SLM pattern.*

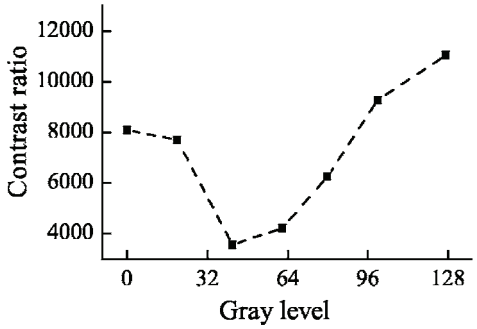

A Young's interference experiment between two selected individual VCSEL emitters is depicted in Fig. 3. NF and FF patterns of the lasing VCSEL array in Figs. 3(a) and 3(b) were acquired while the checkerboard pattern was impressed onto the entire active array of the SLM. The main lasing supermode of the VCSEL array is characterized by out-of-phase emission of neighboring VCSELs, resulting in a NF intensity pattern with maxima located at the VCSEL pixels and zero intensity in between. The FF pattern reveals four principal lobes of constructive interference from all 100 VCSELs. Confining the checkerboard phase modulation to the domains of the two selected VCSEL pixels allows us to selectively image them through the lock-in amplifier. In Fig. 3(c), two such VCSELs are separated by one lattice period and are thus expected to reveal in-phase emission. The Young's interference pattern [Fig. 3(d)] indeed shows a bright interference fringe at the center of the pattern, confirming coherent in-phase emission of the two selected VCSELs. The four principal lobes of the remaining 98 VCSELs are practically invisible, attesting to the high contrast ratio of the lock-in amplifier.

Figure 3(e) shows the FF intensity pattern line scan $I(\theta)$ acquired along the dashed line in Fig. 3(d). By measuring the FF line scans $I_1(\theta)$ and $I_2(\theta)$ of the two solitary VCSELs [Fig. 3(e)] and using the expression $I = I_1 + I_2 + 2\sqrt{I_1 I_2}|\gamma_{12}|\cos\Delta\varphi$, we extract the normalized correlation function $|\gamma_{12}|\cos\Delta\varphi$ [Fig. 3(f)]. Its amplitude, which is independent of I_1 and I_2, measures the degree of mutual coherence $|\gamma_{12}|$. As expected, the instantaneous phases of the two selected VCSELs of Fig. 3(c) are highly correlated, with $|\gamma_{12}| = 0.92$. The deviation from unity is probably due to the contribution of other (lasing or nonlasing) super-modes.

Fig. 3: *(a) Near-field and (b) far-field patterns of the lasing 10 × 10 VCSEL array, (c) NF and (d) FF patterns of two selected VCSEL pixels [the arrows in (a) indicate their row and column positions], (e) FF line scans of the solitary VCSEL pixels (dashed curves 1 and 2) and of the interference pattern of the two VCSELs (solid curve 3) along the dashed line in (d). (f) Normalized correlation function of the selected VCSEL pixels.*

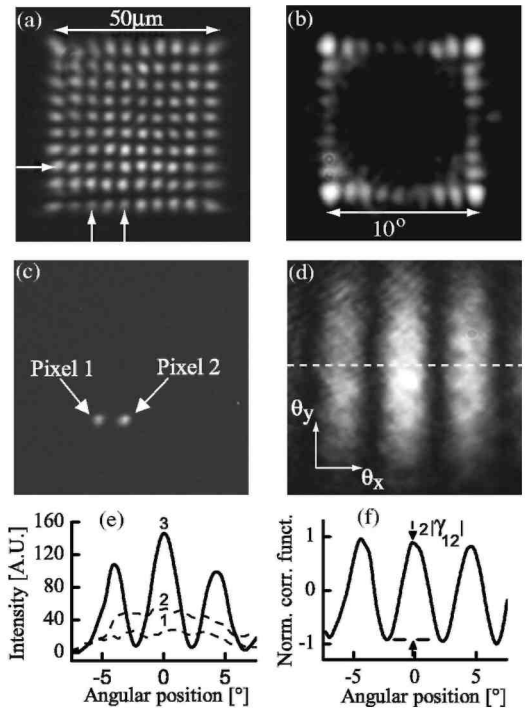

In summary, we have presented a 2D space-domain lock-in amplifier for dynamic aperturing of broad optical beams and selective image extraction. Previously, selective image extraction with a 2D lock-in amplifier was realized using time-domain uniform phase modulation on a primary SLM and subsequent synchronous detection on a secondary SLM. Unfortunately, the contrast of the extracted image pattern was not specified. In our device, the contrast ratio between blocked and transmitted intensity patterns is more than 10,000:1, which is believed to be a record value for liquid-crystal SLMs. We expect that the contrast can be further increased by using SLM cells with higher fill factors. An application of the lock-in amplifier in evaluating the mutual coherence of two selected VCSELs within a phase-locked array was demonstrated.

References

1. L. Hu, L. Xuan, Y. Liu, Z. Cao, D. Li, and Q. Q. Mu, Opt. Express 12, 6403 (2004).

2. V. Bagnoud and J. D. Zuegel, Opt. Lett. 29, 295 (2004).

3. R. L. Eriksen, V. R. Daria, and J. Glückstad, Opt. Express 10, 597 (2002).

4. V. R. Daria, P. J. Rodrigo, and J. Glückstad, Opt. Commun. 232, 229 (2004).

5. Y. Bitou, Opt. Lett. 28, 1576 (2003).

6. P. J. Smith, C. M. Taylor, A. J. Shaw, and E. M. McCabe, Appl. Opt. 39, 2664 (2000).

7. M. Killinger, J. L. de Bougrenet de la Tocnaye, P. Cambon, R. C. Chittick, and W. A. Crossland, Appl. Opt. 31, 3930 (1992).

8. X. Xun and R. Cohn, Appl. Opt. 43, 6400 (2004).

9. S. Shen and A. M. Weiner, IEEE Photon. Technol. Lett. 11, 566 (1999).

10. M. Orenstein, E. Kapon, J. P. Harbison, L. T. Florez, and N. G. Stoffel, Appl. Phys. Lett. 60, 1535 (1992).

11. L. D. Landau and E. M. Lifshits, *Electrodynamics of Continuous Media* (Nauka, 1992), §94.

12. E. Hällstig, T. Martin, L. Sjöqvist, and M. Lindgren, J. Opt. Soc. Am. A 22, 177 (2005).

13. J. A. Davis, D. M. Cottrell, J. Campos, M. J. Yzuel, and I. Moreno, Appl. Opt. 38, 5004 (1999).

14. G. C. Dente, K. A. Wilson, T. C. Salvi, and D. Depatie, Appl. Phys. Lett. 51, 9 (1987).

15. N. W. Carlson, V. J. Masin, M. Lurie, B. Goldstein, and G. A. Evans, Appl. Phys. Lett. 51, 643 (1987).

16. Z. He, N. Mukohzaka, and K. Hotate, IEEE Photon. Technol. Lett. 9, 514 (1997).